
EMPLOYING DISCRETE FOURIER TRANSFORM IN REPRESENTATION LEARNING

A PREPRINT

Raouf HojatJalali

Universit'a di Siena, Italy
mohamm.hojatjalali@student.unisi.it

Edmondo Trentin

DIISM, Universit'a di Siena, Italy
trentin@dii.unisi.it

June 7, 2025

ABSTRACT

Image Representation learning via input reconstruction is a common technique in machine learning for generating representations that can be effectively utilized by arbitrary downstream tasks. A well-established approach is using autoencoders to extract latent representations at the network's compression point. These representations are valuable because they retain essential information necessary for reconstructing the original input from the compressed latent space. In this paper, we propose an alternative learning objective. Instead of using the raw input as the reconstruction target, we employ the Discrete Fourier Transform (DFT) of the input. The DFT provides meaningful global information at each frequency level, making individual frequency components useful as separate learning targets. When dealing with multidimensional input data, the DFT offers remarkable flexibility by enabling selective transformation across specific dimensions while preserving others in the computation. Moreover, certain types of input exhibit distinct patterns in their frequency distributions, where specific frequency components consistently contain most of the magnitude, allowing us to focus on a subset of frequencies rather than the entire spectrum. These characteristics position the DFT as a viable learning objective for representation learning and we validate our approach by achieving 52.8% top-1 accuracy on CIFAR-10 with ResNet-50 and outperforming the traditional autoencoder by 12.8 points under identical architectural configurations. Additionally, we demonstrate that training on only the lower-frequency components—those with the highest magnitudes—yields results comparable to using the full frequency spectrum, with only minimal reductions in accuracy.

Keywords Representation learning · Fourier Transform

1 Introduction

Unsupervised representation learning continues to be a critical challenge in machine learning. Of the many methods developed in this field, three primary approaches introduced by Bengio et al. [1] are particularly notable: the probabilistic models, which infer latent variables to represent the underlying distribution of observed data; geometrically motivated manifold-learning approaches, which are based on the idea that the observed data tend to cluster near a lower-dimensional manifold; and reconstruction-based algorithms such as autoencoders, which compress high-dimensional inputs into compact latent representations while preserving enough information to reconstruct the original input.

Recent advances in self-supervised learning have further expanded the landscape of unsupervised representation learning. The two architectural categories outlined in Ravid Shwartz-Ziv et al. [2] are: generative architectures, where an objective function is used to measure the divergence between input data and predicted reconstructions; and joint embedding architectures, which encode multiple views of input and ensure that the generated representations are informative and mutually predictable.

We introduce Fourier Transform Representation Learning, a method closely related to reconstruction approaches by Bengio et al. [1] and generative architectures by Ravid Shwartz-Ziv et al. [2]. The core idea is to use the DFT of the input

as the learning objective instead of reconstructing the original input. This approach aligns with reconstruction methods because not all these methods aim to reproduce the raw input. A notable example is Transforming Auto-encoders by Hinton et al. [3], where the output is an affine transformation (e.g., translation, rotation, scaling, or shearing) of the input. By treating the DFT as a mathematical transformation of the input, our approach fits within the broader category of reconstruction-based learning. It is also worth emphasizing that the DFT is a lossless transformation (if the entire spectrum is used), which theoretically allows the original input data to be perfectly reconstructed by applying the inverse DFT to the output.

1.1 Natural Images as Input

This study centers on extracting useful representation from images as inputs. An image is constructed as a multi-dimensional numerical array, with each entry representing the intensity of a specific pixel in the image. Consider an image of size H -by- W pixels with C channels (e.g., RGB), this can be represented as an array I of size $C \times H \times W$, where each element $I_{c,h,w}$ denotes the intensity of the pixel at position (h, w) for channel c , as shown in following equation:

$$I \in \mathbb{R}^{C \times H \times W} \quad (1)$$

Particularly, we focus on the natural images, the same category of images studied in Torralba et al. [4]. Natural images are characterized by significant redundancy and statistical regularities. The inherent spatial redundancy in natural images makes DFT a strong candidate for learning targets, as each DFT frequency component is explicitly designed to detect a distinct periodic pattern. Another key statistical property (noted in Torralba et al.) we exploit in our experiments is that the average power spectrum of natural images reduces by $1/f^\alpha$, where f is the spatial frequency. This suggests that natural images are dominated by low-frequency components, allowing training to focus on a subset of these components, as they contain most of the relevant information. This becomes crucial when working with high-resolution images, where using the full frequency spectrum could drastically increase the number of network parameters. In Section 3.4, we present empirical results showing that training with only lower-frequency components yields results comparable to those achieved with the complete frequency spectrum.

1.2 Flexibility in DFT Applications

The DFT offers remarkable flexibility in its application to spatial data, enabling transformations across multiple dimensions either independently or in combination. To understand this, we begin by analyzing the general form of the n -dimensional DFT. Mathematically, it is expressed as following equation:

$$X_{k_1, k_2, \dots, k_n} = \sum_{n_1=0}^{N_1-1} \sum_{n_2=0}^{N_2-1} \dots \sum_{n_n=0}^{N_n-1} \left(x_{n_1, n_2, \dots, n_n} \cdot \prod_{d=1}^n e^{-2\pi i \frac{k_d n_d}{N_d}} \right) \quad (2)$$

where X_{k_1, k_2, \dots, k_n} represents the frequency components, and x_{n_1, n_2, \dots, n_n} is the input image in the spatial domain. The indices k_d and n_d correspond to the frequency and spatial dimensions respectively, while N_d is the size of the d -th dimension. The general form of the DFT is highly versatile, enabling transformations of data across any number of dimensions. It connects the spatial domain with the frequency domain, where periodic structures often appear more defined. The general DFT form on image space can be better understood by decomposing it hierarchically, explicitly demonstrating the connections between its various dimensional components. This becomes apparent when decompose the Equation (2) as following equation:

$$X_{k_c, k_h, k_w} = \sum_{c=0}^{C-1} \left(e^{-2\pi i \frac{k_c c}{C}} \sum_{h=0}^{H-1} \left(e^{-2\pi i \frac{k_h h}{H}} \sum_{w=0}^{W-1} \left(e^{-2\pi i \frac{k_w w}{W}} \cdot I_{c,h,w} \right) \right) \right) \quad (3)$$

This decomposed formulation inherently utilizes the computations of lower-dimensional DFTs. It is evident that the 1D and 2D DFTs are embedded within this structure. This hierarchical structure employs a stepwise method to compute the 3D DFT. By first applying 1D DFTs along one dimension, then using these to compute 2D DFTs, and ultimately combining them for the full 3D DFT result. As we transition from 1D to 2D and finally to 3D, we gradually integrate more dimensions of the image space Equation (1). This hierarchical multi-dimensional DFT method facilitates the generation of tailored learning targets for our experiments. When applying a 1D DFT to rows, the computation is limited to this dimension, which helps detect horizontal frequency patterns while keeping spatial information intact in columns and channels. By scaling this to a 2D DFT across the image's plane, computation is restricted to both rows and

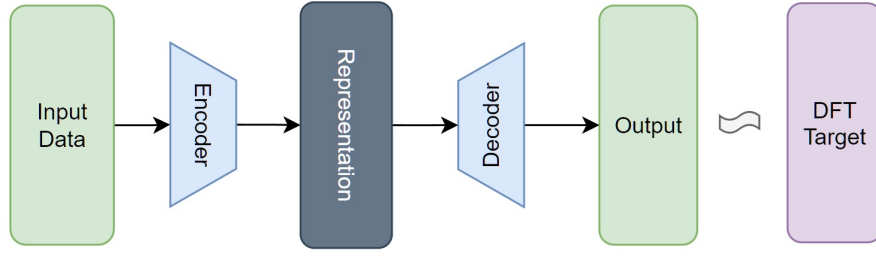


Figure 1: DFT representation learning employs a similar autoencoder architecture to reconstruct frequency components derived from the DFT.

columns, ensuring that channel-specific information remains unaffected. Finally, a 3D DFT incorporates all dimensions, where information is shared across rows, columns, and channels.

2 Fourier Transform Representation Learning

Having explored the mathematical foundations of the DFT and its application to our image space, we now introduce our proposed approach for learning image representation. As shown in Figure 1, the core idea involves using an autoencoder to compress the input into a latent representation. From this compressed form, we reconstruct the DFT frequency components that originated from the input images.

2.1 Learning Objectives

The DFT produces a complex-valued output. As our network outputs real values, we must identify a way to express DFT frequencies in a real-valued form. In addition to real and imaginary parts, frequency analysis typically uses magnitude and phase to describe complex values. If we denote the DFT output as $X[k]$ (where k represents the frequency index across any dimension), we can express the relationship between these components using the following decompositions as shown in following equation:

$$X[k] = \text{Re}(X[k]) + i \cdot \text{Im}(X[k]) = |X[k]| \cdot e^{i \cdot \angle X[k]} \quad (4)$$

Each component isolates a unique aspect of the frequency domain, highlighting different characteristics. The real and imaginary parts, when combined, fully define the complex DFT output, while individually they reflect projections onto their respective axes. The magnitude measures the distance from the origin to the complex point in the plane, signifying the strength, while the phase is the angle from the real axis, reflecting the shift in the periodic pattern captured by a DFT frequency component. To evaluate which components yield more effective learning representations, we defined 6 learning targets:

- **Real Part Only:** Uses only the real part of the frequency domain $\text{Re}(X[k])$ as the target, isolating real-value contributions to learning.
- **Imaginary Part Only:** Uses only the imaginary part of the frequency domain $\text{Im}(X[k])$ as the target, isolating imaginary-value contributions to learning.
- **Real and Imaginary:** Using concatenation of both real and imaginary parts as targets.
- **Magnitude Only:** Uses only the magnitude of frequency components $|X[k]|$ as the target, focusing on strength while ignoring phase.
- **Phase Only:** Uses only the phase information of frequency components $\angle X[k]$ as the target, focusing on shift of the periodic patterns.
- **Magnitude and Phase:** Using concatenation of both magnitude and phase as targets.

2.2 DFT Dimensionality Selection

Building upon the DFT formulation adapted to image space 3, we explored three distinct learning objectives: a 1D DFT applied along the row dimension, capturing horizontal frequency patterns while preserving spatial information in

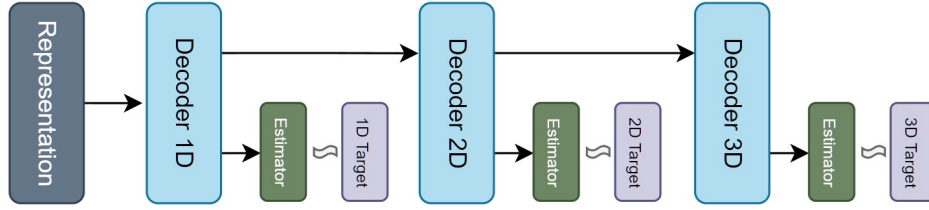


Figure 2: Sequential training approach of different dimensions of DFT.

column and channel dimensions; a 2D DFT covering both row and column dimensions, while maintaining cross-channel information; and a complete 3D DFT encompassing all three dimensions of image space. Each approach represents a different level of frequency information extraction from the input data, allowing us to evaluate the effectiveness of various representation learning based on dimensionality selection of DFT.

Another approach to leveraging the DFT formulation in representation learning involves adopting a sequential strategy. As shown in Figure 2, this method emulates the computational steps of the DFT during training through a multi-stage process, utilizing a series of specialized decoders arranged in sequence. Each decoder estimates a different dimensional aspect of the DFT, with later stages in the sequence building progressively on the outputs of earlier stages.

The sequential training approach features a shared encoder to generate the latent representation. The representation is then processed sequentially through a series of decoders, each consisting of:

1. A representation generator that constructs an intermediate representation passed to the next decoder.
2. A lightweight estimator that maps this intermediate representation to the DFT-specific output for its respective dimension.

2.3 Specific Frequency Components of Interest

As mentioned in Section 1.1, natural images are often characterized by their dominance of low-frequency components in their magnitude distribution. To demonstrate this, we performed a 1D DFT on the row dimension across all images in our dataset—CIFAR-10—as detailed in following equation:

$$A_{k_w} = \frac{1}{N \times C \times H} \sum_{n=0}^{N-1} \sum_{c=0}^{C-1} \sum_{h=0}^{H-1} |X_{c,h,k_w}^{(n)}| \quad (5)$$

where A_{k_w} represents the aggregated value for frequency component k_w , N is the total number of images in the dataset, and $X_{c,h,k_w}^{(n)}$ is the 1D DFT component at frequency k_w for channel c , row h of image n . As shown in Figure 3, the aggregation results display a clear U-shaped trend in the distributions. This pattern reflects higher magnitudes at both ends of the spectrum—where low-frequency components are located—and a gradual decline in magnitude as the spectrum approaches the Nyquist frequency at its center. We utilized this statistical property in our experiments in Section 3.4 by training exclusively on a subset of frequency components. Specifically, we selected the lowest fourth and eighth of the low-frequencies to demonstrate that these subsets still achieve an effective representation compared to using the full spectrum.

3 Experiments

In this section, we explore experiments conducted to evaluate the effectiveness of the Fourier Transform Representation Learning approach. Each experiment is designed to investigate specific aspects of the method, revealing how the learned representation is shaped and utilized for downstream tasks.

In order to evaluate the learned representations, we applied the linear evaluation protocol outlined in VICReg [5]. This protocol freezes the encoder’s parameters and trains a linear classifier connected to the encoder. Unlike the pretraining phase, which did not utilize CIFAR-10 labels, we used these labels during a 3-epoch classification training and report Top-1 and Top-5 accuracies.

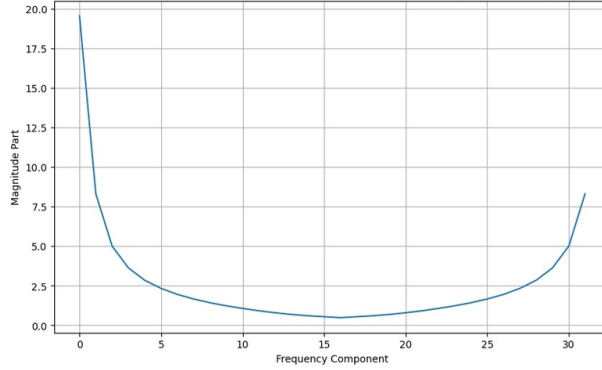


Figure 3: Aggregated magnitude spectrum across all rows of all images in the CIFAR-10 dataset.

3.1 Learning Objectives Experiments

Here we examined different target formulations derived from the 1D DFT across the row dimension. As highlighted in Section 2.1 these experiments focuses on identifying which DFT-derived target representations generate the most effective learned representations, based on the linear evaluation protocol described earlier. As shown in Table 1, across six different DFT target formulations, the Magnitude representation is the most effective for representation learning. The Magnitude-only experiment achieved the highest validation Top-1 accuracy of 43.92% and Top-5 accuracy of 88.57%, significantly outperforming all other target formulations. For future experiments, we will exclusively use the Magnitude representation as our DFT target, as it provides the optimal performance based on our evaluation metrics.

Table 1: Performance Comparison of Different DFT Target Formulations

DFT Target	Acc@1[V]	Acc@5[V]	Acc@1[T]	Acc@5[T]	Epoch(sec)
Real Part	40.78	86.63	45.62	89.76	103.90
Imaginary Part	34.99	82.93	41.65	87.32	107.00
Real + Imaginary	40.12	85.97	44.88	89.28	111.96
Magnitude	43.92	88.57	49.85	91.62	105.37
Phase	33.99	82.20	39.41	86.44	107.87
Magnitude + Phase	42.41	87.84	48.31	90.90	111.13

3.2 DFT Dimensionality Selection Experiments

In the DFT Dimensionality Selection experimental design, we systematically examined how varying the dimensionality of the DFT impacts the quality of learned representations. Building on the theoretical foundations outlined in Section 2.2, we analyzed three distinct approaches: a 1D DFT applied along the row dimension, a 2D DFT incorporating both row and column dimensions, and a full 3D DFT encompassing all three dimensions. As shown in Table 2, the 2D DFT configuration achieves superior performance compared to 1D and 3D approaches across all accuracy metrics, with the highest validation and training accuracies for both Top-1 and Top-5 measurements. Notably, the 3D DFT, although incorporating additional dimensional information, performs worse than both 1D and 2D methods. This suboptimal performance attributes to the inherent differences between row/column and channel dimensions. While row and column exhibit strong spatial correlations and structural patterns—features that frequency transformations can effectively leverage—the channel dimension lacks these intrinsic spatial relationships.

Table 2: Performance Comparison of Different DFT Dimensionalities

DFT Dim	Acc@1[V]	Acc@5[V]	Acc@1[T]	Acc@5[T]	Epoch(sec)
1D (Width)	43.92%	88.57%	49.85%	91.62%	105.37
2D (Width+Height)	45.68%	90.09%	52.46%	93.10%	103.77
3D (All dimensions)	42.56%	88.47%	49.47%	91.78%	105.74

3.3 Sequential Training Experiments

As outlined in Section 2.2, we discussed a different approach to estimate the DFT targets which decomposes the multi-dimensional DFT estimation into distinct steps using a series of specialized decoders arranged sequentially. As shown in Table 3, the sequential 2D DFT approach achieves a slight improvement over its non-sequential counterpart, with a validation accuracy of 46.05% (Top-1) compared to 45.68% for the non-sequential version. This small gain indicates that the sequential construction of the frequency domain through specialized decoders enhances the model’s representational capacity. However, this benefit comes at a significant computational cost, as the sequential method requires considerably more computational resources than the non-sequential approach.

Table 3: Performance Comparison of DFT Sequential Training

DFT Dim	Acc@1[V]	Acc@5[V]	Acc@1[T]	Acc@5[T]	Epoch(sec)
1D (non-seq)*	43.92%	88.57%	49.85%	91.62%	105.37
2D (non-seq)*	45.68%	90.09%	52.46%	93.10%	103.77
2D (seq)	46.05%	90.31%	52.80%	93.23%	165.36
3D (seq)	43.61%	89.42%	50.05%	92.45%	231.51

3.4 Selective Frequency Components Experiments

Building upon the use of a subset of frequency components as learning targets discussed in Section 2.3, we implemented two selective frequency approaches to systematically evaluate their impact on representation learning and downstream task performance. We experimented with using one-quarter of the frequency components in the 1D DFT, followed by a similar setup involving one-eighth of the frequency components in the 1D DFT. As shown in Table 4, using the full frequency spectrum yields the best performance across all accuracy metrics. While the full 1D DFT approach achieved the highest validation accuracies, the quarter-spectrum approach results in a modest drop (approximately 2 percentage points in Top-1 validation accuracy), and the eighth-spectrum approach exhibits a similar decline. Notably, both selective approaches—despite using only 25% or 12.5% of the frequency components—achieve relatively competitive accuracy, with less than a 5% relative drop in Top-1 validation accuracy compared to the full spectrum approach.

Table 4: Performance Comparison of Frequency Selectivity

DFT Dim	Acc@1[V]	Acc@5[V]	Acc@1[T]	Acc@5[T]	Epoch(sec)
1D Full Spectrum*	43.92%	88.57%	49.85%	91.62%	105.37
1D Quarter Spectrum	41.93%	87.80%	47.82%	90.98%	104.28
1D Eighth Spectrum	41.91%	87.80%	47.07%	90.74%	101.69

*Tested in previous section

3.5 Comparative Representation Learning Experiments

In this section, we conducted experiments comparing our Fourier Transform Representation Learning approach with standard autoencoders, a natural baseline since they learn compact representations through encoding and decoding processes. As shown in Table 5, the sequential 2D DFT method, our most effective Fourier Transform approach, achieved a validation accuracy of 46.05% (Top-1) and 90.31% (Top-5). This performance significantly outperforms the standard autoencoder, which achieved 35.29% (Top-1) and 83.75% (Top-5) validation accuracy. The notable 10.76 percentage point gap in Top-1 accuracy suggests that our frequency domain transformation approach captures more discriminative features than standard reconstruction-based representations.

Table 5: Performance Comparison of Different Representation Learning Methods

Method	Acc@1[V]	Acc@5[V]	Acc@1[T]	Acc@5[T]	Epoch(sec)
Autoencoder	35.29%	83.75%	39.99%	86.71%	80.48
2D DFT (non-seq)	45.68%	90.09%	52.46%	93.10%	103.77
2D DFT (seq)	46.05%	90.31%	52.80%	93.23%	165.36

3.6 Implementation Details

In this section, we outline the implementation details for Fourier Transform Representation Learning. The dataset used is CIFAR-10 [7], with labels removed. The architecture follows a setup similar to that described in VICReg [5], featuring a ResNet-50 [6] encoder with 2048 output units. The decoder comprises three fully-connected layers, each paired with batch normalization, and is designed to produce outputs with the same dimensionality as DFT targets. For the loss function, we compute the squared differences between the model’s outputs and the DFT targets.

4 Conclusion

The paper presented the Fourier Transform Representation Learning, a different reconstruction-based approach compared to standard Autoencoders. We discovered that among the various possible DFT target formulations, the magnitude representation emerged as consistently superior learning target. Next, we investigated DFT dimensionalities and found that a 2D DFT implementation—combining row and column dimensions—delivered the best performance. Our investigation into sequential training of multi-dimensional DFT revealed further nuances. By breaking down multi-dimensional DFT computation into multiple steps with specialized decoders arranged in sequence, we observed modest performance improvements for the 2D implementation. Our final series of experiments explored selective frequency components, motivated by the observation that natural images typically exhibit higher magnitudes on low-frequency components. We found that using the complete frequency spectrum still yielded the best performance, outperforming selective approaches that focused on only one-quarter or one-eighth of the frequency components. This suggests that while lower frequency components do contain significant information, higher frequency components still contribute meaningful information for representation learning that benefits downstream classification tasks. Nevertheless, it’s remarkable that despite using only a fraction of the frequency components, both selective approaches achieved competitive accuracy with less than a 5% relative drop in Top-1 validation accuracy compared to the full spectrum approach. When comparing our DFT-based approach with established representation learning methods, we found that our best performing model—sequential 2D DFT—significantly outperformed standard autoencoders by over 10 percentage points in Top-1 accuracy.

References

- [1] Yoshua Bengio and Aaron Courville and Pascal Vincent. Representation Learning: A Review and New Perspectives. 2014.
- [2] Ravid Shwartz-Ziv and Yann LeCun. To Compress or Not to Compress- Self-Supervised Learning and Information Theory: A Review. In *arXiv preprint arXiv:2304.09355*, 2023.
- [3] Geoffrey Hinton, Alex Krizhevsky, and Sida Wang. Transforming Auto-Encoders. In *Artificial Neural Networks and Machine Learning – ICANN 2011*, volume 6791, pages 44–51, 2011.
- [4] A. Torralba and A. Oliva. Statistics of natural image categories. In *Network (Bristol, England)*, volume 14, pages 391–412, 2003.
- [5] Adrien Bardes and Jean Ponce and Yann LeCun. VICReg: Variance-Invariance-Covariance Regularization for Self-Supervised Learning. In *CoRR*, volume abs/2105.04906, 2021.
- [6] Kaiming He and Xiangyu Zhang and Shaoqing Ren and Jian Sun. Deep Residual Learning for Image Recognition. In *2016 IEEE Conference on Computer Vision and Pattern Recognition (CVPR)*, pages 770–778, 2016.
- [7] Alex Krizhevsky. Learning Multiple Layers of Features from Tiny Images. In . , 2009.
- [8] Jia Deng and Wei Dong and Richard Socher and Li-Jia Li and Kai Li and Li Fei-Fei. ImageNet: A large-scale hierarchical image database. In *2009 IEEE Conference on Computer Vision and Pattern Recognition*, pages 248–255. IEEE, 2009.